

Enzyme Immobilization on a Delignified Bamboo Scaffold as a Green Hierarchical Bioreactor

Yihua Ren,[§] Libo Zhang,[§] Tao Sun, Yingwu Yin,^{*} and Qian Wang^{*}Cite This: <https://doi.org/10.1021/acssuschemeng.2c00346>

Read Online

ACCESS |



Metrics & More



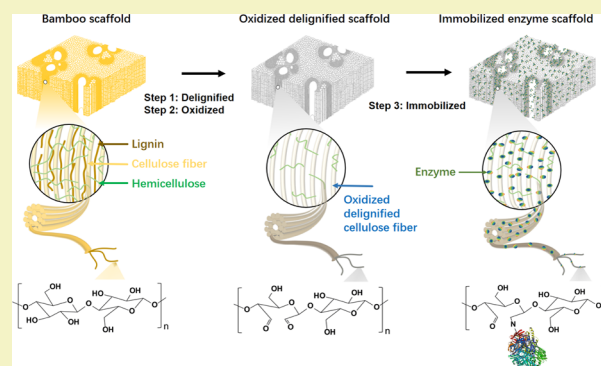
Article Recommendations



Supporting Information

ABSTRACT: Enzymes immobilized on cellulose-based supports provide important applications because they are convenient, economical, and stable. In this paper, we report the application of delignified bamboo as a novel cellulose-based scaffold for enzyme immobilization and bamboo enzyme-based flow bioreactors, which can drastically improve the catalytic reaction and subsequent separation. The delignified bamboo provides a superior biobenevolent and hierarchically structured platform that can be conveniently derivatized to conjugate functional proteins with high loading capacity. With an optimized delignification process and a modified Schiff base-dependent conjugation method, we identified an efficient approach to immobilize enzymes on bamboo. In our system, generally $\sim 8 \text{ mg/m}^2 \cdot \text{g}^{-1}$ proteins can be immobilized on the delignified bamboo, which is significantly higher than that of the reported methods. The immobilized enzymes on bamboo showed sustained activity under ambient conditions, excellent reusability with 13 cycles, and high stability of more than 7 weeks of storage at 4 °C, which can be readily adapted in flow reactors for both single transformation and tandem catalysis. As an example, drugs of abuse in synthetic urine samples were analyzed in β -glucuronidase (BGU)-functionalized flow reactors in 0.1 M phosphate buffer, pH 7.4, at room temperature, the condition suitable for the bioanalysis. Our work demonstrates that the delignified bamboo can serve as a readily available support for enzyme immobilization and hierarchical bioreactor construction, which will potentially increase the robustness of enzymes in analytical and synthetic applications.

KEYWORDS: delignified bamboo, cellulose, enzyme immobilization, flow reactor, β -glucuronidase, multienzyme reaction



INTRODUCTION

Enzymes, as efficient biocatalysts in versatile reactions, have been widely explored and used in biotechnological sciences and synthetic applications.^{1,2} Despite significant advantages compared to chemical catalysts including high specificity and high efficiency,³ the practical applications of enzymes are often hampered by their high cost that is mainly caused by the requirement of production systems and complicated purification processes, low stability under non-native conditions, and inefficient reusability.^{4,5} Enzyme immobilization represents a practical way to overcome these limitations and obtain more stable, active, and reusable biocatalysts. With some well-designed systems, the enzymes' activity, substrate selectivity, thermal stability, and organic solvent tolerance could be improved, highlighting the benefit of enzyme immobilization for synthetic applications.^{6–8} Generally, nonsophisticated equipment is required for enzyme immobilization,⁹ and a variety of materials and chemistries have been explored for enzyme immobilization so far.^{10,11} Specific requirements, such as the cost of the materials, harmlessness to both health and the environment, resistance to chemical and microbial decomposition, effectiveness of the immobilization process,

effect on the catalytic efficiency, and facilitation of the operation process, should be considered to design an effective immobilization system.^{12,13}

The materials that have been successfully employed as supports include carbon nanotubes (CNTs),¹⁴ metal–organic frameworks (MOFs),¹⁵ synthetic and natural polymers,^{11,16,17} hydrogels,¹⁸ zeolites,¹⁹ other inorganic particles,²⁰ etc. Among them, cellulose,²¹ as a natural hydrophilic material, is one of the most promising supports for enzyme immobilization. Because of its tight packing (i.e., crystallite) resulting from the inter- and intramolecular hydrogen bonds,²² cellulose is normally dissolved by certain specialized solvents (e.g., NaOH/thiourea/urea, 4-methylmorpholine *N*-oxide, lithium chloride/dimethylacetamide) and then precipitated in a swollen form for derivatization.^{12,23} This process requires

Received: January 17, 2022

Revised: April 16, 2022

volatile and harmful organic solvents and has been considered energy-intensive. On the other hand, cellulose supports are often packed into a fixed bed,²⁴ which are limited by mass-transfer resistances,²⁵ intolerance of high pressure,²⁶ inhomogeneous distribution of reactants and products, and poor reproducibility.²⁷ Thus, the search for a more sustainable method for cellulose's application in enzyme immobilization is continuously desirable and essential.

Compared to the 10–20 years of the life cycle of timber, bamboo only needs 3–5 years. Bamboo yields up to 25-fold more materials due to fast growth (i.e., up to 100 cm/day), sequesters fourfold more carbon dioxide, and releases 35% more oxygen than wood. Bamboo cell walls are hierarchical assemblies of different types of fibrils including macrofibrils, microfibrils, and elementary fibrils.^{22,28} Bamboo offers a significant and sophisticated structure with parenchymal cells as the matrix and vascular bundles as reinforcement. These hierarchical structures provide various pores with different sizes and make bamboo an excellent cellulose-based support.

The bamboo or wood monolith with different modifications has been used in industrial applications.^{29,30} In addition to cellulose nanofiber extraction and application, the porosity of the hierarchical structure with fast mass transfer and high permeability has been explored.³¹ Most lignin in cell walls can be removed through the delignification process,³² while the overall morphology and cellular structure can be preserved.³¹ The delignification process also increases the internal multiscale porosity vastly and enables facile derivatization due to the abundance of hydroxyl groups exposed.³³ The highly aligned cellulose fibers exhibit excellent liquid transport capacity,^{34,35} leading to a high water flux in bamboo. Therefore, the scaffold is chemically amenable for enzyme immobilization due to the abundant reactive groups and hydrophilic chains and dynamically suitable for catalysis.^{28,30} By taking advantage of the multiscale porosity of the internal structure, the delignified bamboo can also be used for separation applications.³⁰

To date, both covalent and noncovalent strategies have been explored to immobilize enzymes on a cellulose scaffold and other solid supports.^{36–39} Multiple types of interactions and multipoint interactions could occur during and after the protein immobilization,^{40–44} which should be considered for the design of the immobilization method and process optimization.^{45,46} The amine groups at the side chain of lysine residues and the N-terminal of the proteins are commonly used for enzyme immobilization since the majority of proteins have such amine groups on their surface, which are usually exposed to medium and accessible for derivatization.⁴⁰ The amine group can react with the aldehyde group of the oxidized cellulose unit to form a Schiff base.^{47,48} However, the Schiff base is not stable, while once reduced to the C–N bond, the formed alkylamine linkage is highly stable.⁴⁹ Cyanoborohydride instead of sodium borohydride was chosen to serve as a milder reducing agent, which has been reported to successfully preserve the function of antibodies.^{50,51} With this method, the protein can be feasibly functionalized on the hierarchical bamboo scaffold with a minimized spacer arm. Compared to the reported methods utilizing affinity tags and nanoparticles for mediation,^{12,52,53} lower steric hindrance and significantly improved atom economy were achieved in our system.

(β)-glucuronidase (BGU) has been extensively used in research and analytical laboratories to hydrolyze steroid β -glucuronides and steroid conjugates (glucuronides).^{54–56} Different bioanalytic methods with the BGU-based hydrolysis

reaction as the initial step were extensively applied in drug metabolism studies.⁵⁶ For example, the enzyme has been applied to prepare samples for liquid chromatography–mass spectrometry (LC-MS), immunoassay, and other analytical analyses.⁵⁷ In these assays, the protein needs to be removed after the enzymatic reaction to achieve high sensitivity and accuracy. The process is tedious and may bring variations. BGUs contain several notable secondary structural forms (i.e., jelly roll barrel and a triose-phosphate isomerase (TIM) barrel)⁵⁸ and show excellent stability and hydrolytic activity under ambient conditions due to the qualitative S_N2 reactions involved in the catalysis.⁵⁹ The activity of BGUs can be tuned by the molecular lipophilicity and polarity and the exterior environment.⁵⁵ All these factors make BGUs a useful but also a challenging target for enzyme immobilization. In addition, BGU immobilization on the functional group-abundant materials could potentially separate the enzyme from the raw materials, prevent enzyme leaching, and improve the stability of the tertiary structure.^{43,45,60}

In this work, we employ BGU as a model enzyme for immobilization and activity characterization. We also developed a flow bioreactor to enable the enzyme to be used in different analytical applications. Then, we applied our system for tandem catalysis by employing a bienzyme catalyst model, glucose oxidase (GOx) and horseradish peroxidase (HRP). In this contribution, bamboo-based bioreactors are prepared by a facile and cost-effective top-down method, which avoided the energy-consuming process of cellulose fiber extraction, while the natural structure of bamboo and the enzymes' function were well-maintained. We demonstrated that bamboo could serve as a good support for enzyme immobilization and the bamboo-based bioreactors can potentially be used for bioseparation and other enzymatic applications.

EXPERIMENTAL SECTION

Materials. Moso bamboo was collected from the Wuyishan bamboo forest in China. One- to two-year-old bamboo culms were selected. The epidermal and endodermal layers were removed, and the culms were immersed in hydrogen peroxide (H₂O₂, 30%) at 70 °C overnight. Samples were cut to dimensions of 5 mm × 6.5 mm × 25 mm (longitudinal × radial × tangential), and the pieces were stored at 20 °C/65% relative humidity before treatment. BGU (50 kU/mL, 1.0 mg/mL), which was highly purified, filter sterilized, and genetically modified, was provided by Integrated Micro-Chromatography Systems, Inc (Irmo). Horseradish peroxidase (HRP) was purchased from VWR. 2,2'-Azino-bis(3-ethylbenzothiazoline-6-sulfonic acid) diammonium salt (ABTS, C₁₈H₁₈N₄O₆S₄·(NH₃)₂) and 4-nitrophenyl- β -D-glucuronide (pNPG, C₁₂H₁₃NO₉) were purchased from Chem-Impex. Glucose oxidase (GOx), bovine serum albumin (BSA), *i*-propanol (C₃H₈O), glycine (C₂H₅NO₂), and sodium hydroxide (NaOH) were purchased from Sigma. Sulfuric acid (H₂SO₄, 98%), glacial acetic acid (HAc), D-glucose, hydroxylamine hydrochloride (NH₂OH·HCl), sodium cyanoborohydride (NaCNBH₃), and fluorescein-5-maleimide were purchased from Fisher Scientific. Hydrogen peroxide (H₂O₂, wt 30%) was purchased from Macron Fine Chemicals. 4-Nitrophenol (pNP) was purchased from Aldrich. Milli-Q water deionized using a Synergy Ultraviolet (UV) Water Purification System was used in this work. All chemicals and solvents used were of analytical grade. Unless otherwise noted, 0.1 M potassium phosphate, pH 7.4, was used as a buffer.

Delignification Procedure. The moso bamboo pieces were immersed in a beaker with an equal-volume mixture of H₂O₂ solution and HAc for 6 h at room temperature. The mixture was heated at 80 °C until the pieces were becoming totally white from yellow, and the white pieces were immersed in H₂SO₄ aqueous solutions (wt 3%) at 96 °C for 2 h. Then, the delignified bamboo scaffolds were washed

thoroughly using water before use. The samples were stored in water and cut into cylinder shapes with a diameter of 5 mm and a height of 5 mm ($22 \text{ mg} \pm 2 \text{ mg}$). The delignified bamboo scaffold was placed on the bottom of a plastic column, and the device was used for the following experiments.

Characterization of Delignified Bamboo. Brunauer–Emmett–Teller (BET) measurements were carried out on a Micromeritics TriStar II 3020 instrument through a N_2 physisorption surface at a relative pressure between 0.01 and 0.99. The bamboo and delignified bamboo scaffold samples were dried in an oven at 100°C ; then, attenuated total reflection–Fourier transform infrared (ATR-FTIR) spectroscopy was performed at room temperature across the frequency range of $4000\text{--}650 \text{ cm}^{-1}$ on a spectrum system (IS 50, Thermo Nicolet Ltd.), with 64 FTIR scans per spectrum. The surface morphology of the delignified scaffold was observed using a Tescan Vega 3 SBU variable-pressure scanning electron microscopy (SEM) system after gold sputtering (240 s to give an $\sim 40 \text{ nm}$ gold conductive layer; Denton Desk II sputter coater). The porosity of bamboo was determined using the gravimetric method.⁶¹ Specifically, a piece of the scaffold was lyophilized (Labconco Freeze Dryers FreeZone 4.5 Liter) at -80°C with 0.003 MPa vacuum overnight and subsequently weighed using an analytical balance (Denver Instrument PI series). The sample was fully immersed in *i*-propanol for 1 day for complete alcohol infiltration. Then, the sample was cleaned to remove residue from the surface and weighed. The porosity (n) was estimated using eq 1

$$n = \frac{V_{\text{pore}}}{V_{\text{total}}} = \frac{m_{\text{IPA}}/\rho_{\text{IPA}}}{V_{\text{total}}} \quad (1)$$

where V , m , and ρ are the volume, mass, and density, respectively, and IPA indicates *i*-propanol. Three independent measurements were performed on each sample.

The pore structure of the delignified bamboo scaffold after lyophilization was evaluated by mercury penetration using an Autopore IV 9500 mercury intrusion porosimeter (Micromeritics) with the contact angle employed as 130° and measuring range as 0.005–800 μm .

Preparation of the Oxidized Bamboo Scaffold (OBS). The oxidized bamboo scaffold was prepared by the sodium periodate oxidation method.^{47,62} First, the bamboo scaffold was washed with 100 mL of Milli-Q water at a speed of 20–25 mL/min and then immersed in 500 μL of sodium periodate (0.2 M) for 2 h. The whole process was performed in the dark at room temperature with gentle shaking. After oxidation, the excess IO_4^- and Na^+ were removed by washing with around 600 mL of flowing Milli-Q water with 20–25 mL/min. Then, OBS was lyophilized to test the aldehyde amount by deduction from the quantitative reaction with $\text{NH}_2\text{OH}\cdot\text{HCl}$.⁶³ In a typical experiment, two pieces of OBS were reacted with 20 mL of 0.25 M $\text{NH}_2\text{OH}\cdot\text{HCl}$ solution for 3 h at room temperature. The pH of the hydroxylamine solution alone and that with OBS were initially 3.2. After 3 h, the pH of the whole mixture decreased due to HCl release. The solution was then titrated with 0.01 M NaOH solution back to pH 3.2, and the content of CHO was calculated by the following eq 2

$$\text{content of CHO } (\mu\text{mol/mg}) = \frac{V_{\text{eq}} \times C_{\text{NaOH}}}{m} \quad (2)$$

where V_{eq} is the volume (mL) of the standard NaOH solution added to reach pH 3.2, C_{NaOH} is the concentration (mol/L) of the standard NaOH solution, and m (mg) is the weight of OBS.

Immobilization of BSA and BGU. To determine the immobilized capacity, BSA labeled with fluorescein-5-maleimide (F-BSA) was prepared for the test. Specifically, BSA was reacted with fluorescein-5-maleimide overnight at 4°C at a ratio of 1:2 in the dark, and then, the nonreacted fluorescein was removed by dialysis using a dialysis tube with 10 kDa cutoff. During the dialysis procedure, the dialysis buffer with at least 300 times the volume of the sample was used; the dialysis buffer was changed every 6 h three times, and the UV absorbance of the solution at 498 nm before and after labeling

was detected by spectrophotometry (Nanodrop 2000c, Thermo Scientific). F-BSA was protected from light and stored at 4°C . The amount of immobilized protein was measured by detecting the difference between the initial and final concentrations of F-BSA using fluorescence spectrophotometry at 518 nm with the excitation wavelength of 494 nm before and after the Schiff base reaction (Varian Cary Eclipse, Agilent). The F-BSA solution was tested as a negative control at the same time. F-BSA at 0.1, 0.4, and 1.0 mg/mL concentrations was used for optimization of the immobilization conditions. The immobilized scaffold was washed in $5 \text{ mL} \times 1.5 \text{ mL}$ of phosphate buffer (0.1 M, pH 7.4) to get rid of the nonspecifically bound proteins, during which the buffer was changed at 1, 3, 8, 24, and 54 h. The loading amount of the immobilized enzyme was calculated by eq 3

$$\text{loading amount (mg/g)} = \frac{(W_0 - W_t)}{m} \quad (3)$$

where W_0 is the loading amount of enzyme before washing (i.e., after the Schiff base reaction for 16 h), W_t is the accumulated amount of enzyme in the washing solution, and m is the weight of the scaffold.

For BGU immobilization, the OBS samples were immersed in the BGU solution (1.0 mg/mL, 500 μL in 0.1 M, phosphate buffer, pH 7.4); 3 mg of NaCNBH_3 was added, and the mixture was reacted at 4°C for overnight to maximize the protein loading. Finally, the immobilized scaffold was immersed in 1.5 mL of 1.0 mol/L glycine solution for 6 h and then immersed in $5 \text{ mL} \times 1.5 \text{ mL}$ of phosphate buffer as described above to wash away the nonspecifically bound BGUs. Similarly, the loading amount of BGUs was calculated by measuring UV absorbance at 218 nm before and after washing.

The theoretical maximum loading capacity was related to the specific surface area (S) of the delignified bamboo scaffold, which was $0.45 \text{ m}^2/\text{g}$. The theoretical maximum specific adsorption capacity was calculated by eq 4 with an assumption that the enzyme acts like a spherical nanoparticle with a radius of 2 nm

$$\text{theoretical loading capacity (mg/g)} = \frac{S \times M_{\text{enzyme}}}{\pi r^2 N_A} \quad (4)$$

where S is the specific surface area of OBS, M_{enzyme} is the molecular weight of the enzyme (67 kDa for the model protein F-BSA, 80 kDa for the BGU in the monomer form), r is the radius of the enzyme (2 nm), and N_A is Avogadro's number (6.02×10^{23}).

Measurement of BGU Activity and Kinetic Study. The BGU is stable for up to 3 h at incubation temperatures of up to 60°C in the range of pH (4–10).⁶⁴ However, when using different percentages of organic solvents, a correction factor should be applied to the enzyme activities. In this work, we focus on the ambient conditions that were commonly used for BGU application. BGU showed different catalytic activities toward different glucuronidated substrates. In our work, pNPG was used as a representative substrate for enzyme activity evaluation. The concentration of the pNP product was determined by monitoring the absorbance at 400 nm using the method described by Collins et al.⁶⁵ In brief, 500 μL of pNPG (2.0 mM, dissolved in 0.1 M phosphate buffer, pH 7.4) was added to the device containing the immobilized BGU on OBS (BGU@OBS) and incubated at room temperature under static and shaking conditions. The product pNP solution was tested in a nanodrop at different reaction times. To test the reusability and storage stability of BGU@OBS, after the reaction, the BGU@OBS was washed with 100 mL of water and prepared for the next cycle of the test. Three independent replicates were performed under the same conditions. The Michaelis constant, K_m , and v_{max} of free and BGU@OBS were determined using a plate reader. The substrate concentration was set from 0.01 to 2.0 mM. To obtain BGU@OBS with different amounts of immobilized BGUs (20, 10, and 5 μg), the same BGU@OBS blocks were cut into 4, 8, and 16 splits in the growth direction, respectively.

Flowing Biocatalysis. For immobilized BGUs, one scaffold was placed in the sample holder, and the flow rate of pNPG samples (4, 80 μM , 2.0 mM in 0.1 M phosphate buffer, pH 7.4) was constant (5, 25, 50 $\mu\text{L}/\text{min}$) and controlled using a Legato 180 syringe pump (KD

Scheme 1. Illustration of the Bamboo Scaffold Preparation and Protein Immobilization Processes

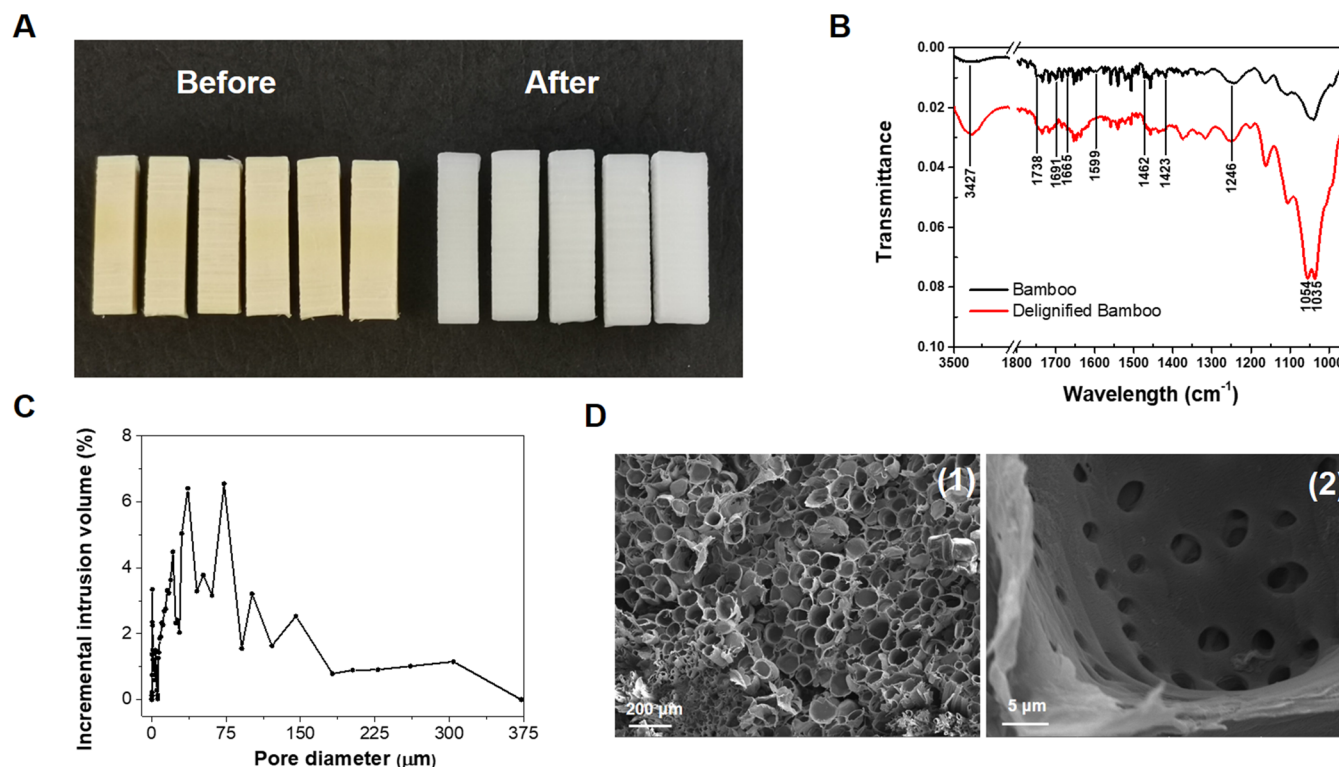
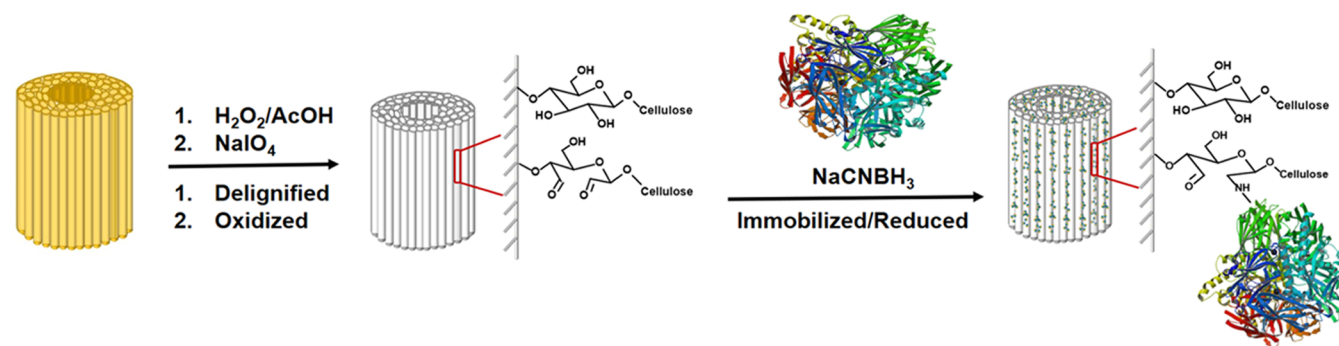


Figure 1. (A) Photo of the bamboo scaffold before and after delignification. (B) ATR-FTIR spectra of the bamboo scaffold before and after delignification. (C) Pore size distribution curve of the delignified bamboo scaffold obtained by mercury intrusion porosimetry. (D) SEM images of cross sections (1) and parenchymal cells (2) of the delignified bamboo scaffold.

Scientific). The flow-through was collected and then tested for UV absorbance at 400 nm. The activity of BGU@OBS was tested after storage for 0 and 2–49 days. To test the hydrolysis of glucuronidated drugs of abuse in synthetic urine (Surine), three kinds of benzodiazepine drugs (oxazepam, lorazepam, temazepam) were used. A spiked Surine mixture (glucuronides: 23.8 ppb, internal standard: 4.76 ppb) was prepared freshly, and the flow-through reaction was executed by mounting one piece (diameter: 5.5 mm, height: 5 mm) of BGU@OBS. The flow rate was controlled to be constant (5, 10, 50 $\mu\text{L}/\text{min}$). Fractions of the sample with 250 μL was collected, quenched using 160 μL of elution solvent (5% FA in MeOH), transferred to a b-Gone Plus Plate, centrifuged at 500g for 1 min, transferred at a volume of 200 μL into separate wells, and diluted into 600 μL . The final samples were analyzed by liquid chromatography–mass spectrometry (LC-MS). Four controls were characterized in parallel: (1) blank scaffold under static conditions, (2) BGU@OBS under static conditions, (3) free BGU, and (4) unhydrolyzed sample (Surine sample only). For the flow reaction with immobilized HRP and GOx, the reactor was executed by mounting two pieces of immobilized GOx on OBS (GOx@OBS), followed by

two pieces of immobilized HRP on OBS (HRP@OBS). The substrate solution came into contact with immobilized GOx first and thereafter was transported to the immobilized HRP. The flow rate was set as 10 $\mu\text{L}/\text{min}$, and the UV absorbance of the ABTS⁺ product was measured at 415 nm. The substrate contains D-glucose (50 mM) and ABTS (2 mM) in phosphate buffer (0.1 M, pH 7.4).

RESULTS AND DISCUSSION

Principle of the Bamboo Cellulose-Based Bioreaction Separator Design. The processing route from native bamboo to protein-immobilized bamboo is depicted schematically in Scheme 1. We first fabricated the delignified bamboo scaffold in a green route using H_2O_2 –HAc.⁶⁶ This mild process employing peracetic acid (PAA) generated from an HAc and H_2O_2 mixture⁶⁷ can delignify bamboo efficiently with little fiber damage. In the process, the bamboo bulk was treated with H_2O_2 –HAc (V:V = 1:1) solution at 80 °C. Mechanical stirring was avoided. The reagents used in the method only contain C, H, and O and do not introduce additional spacer atoms, which

is helpful for the subsequent cellulose oxidation reaction. The hydroxyl group at C2 and C3 of the unit of surface cellulose was oxidized by NaIO_4 to form dialdehyde,^{47,62} which could react with the amino group ($-\text{NH}_2$) on the protein via the Schiff base reaction and be reduced into an alkylamine linkage subsequently in one pot by NaCNBH_3 .

Delignification and Characterization. As shown in Figure 1A, after delignification, the bamboo turned white from slight yellow. An efficient delignification process is critical for the bamboo's application as a support for enzyme immobilization since many enzymes' functions can be tuned by the hydrophobicity of the supports and the polarity of the environment.⁴⁵ The ATR-FTIR spectral analysis (Figure 1B) indicated an effective delignification process. The specific split peaks at 1054 and 1035 cm^{-1} were attributed to cellulose-I and cellulose-II, respectively. The removal of lignin was confirmed by the absence of bands at 1599, 1423, and 1462 cm^{-1} , which were assigned to aromatic skeletal vibrations and C–H deformation combined with aromatic ring vibrations.⁶⁸ The obvious reduction in the intensity of peaks at 1691 and 1655 cm^{-1} was related to carbonyl stretching vibrations in lignin.^{69,70} Partial hemicellulose removal was found based on the disappearance of the peak at 1738 cm^{-1} corresponding to the carbonyl stretching vibration of hemicellulose, and the small change of the absorption peak at approximately 1246 cm^{-1} was due to the C–O linkage in xylan.^{68,71,72} The predominant absorption at 3427 cm^{-1} was assigned to –OH stretching because the cellulose portion was exposed significantly after the removal of lignin and hemicellulose, which could lead to increasing interactions via hydrogen bonding.

After delignification, the density of bamboo decreased from 0.68 ± 0.06 to 0.25 ± 0.01 g/cm^3 (Figure S1). The loss of hemicellulose and lignin contributed to a mass loss of 63% after the process. The porosity of the scaffold increased from 31 ± 4 to $86 \pm 3\%$ (eq 1 and Figure S1). The pore size distribution results (Figure 1C and Table S1) showed that the hierarchical delignified bamboo includes vessels and sieve tubes having the largest conduit pores with a size of 50–120 μm diameter (20%), parenchyma cell lumen with a medium size of 10–50 μm (46%), and the smallest pores in the inner cell wall with a size range of 0.5–10 μm (24%), which is consistent with reported results.^{73–75} The SEM images of raw bamboo and the delignified bamboo scaffold (Figure S2A,B) show that the micropores were exposed significantly after delignification. SEM analysis (Figures 1D(1) and S2B,C) showed vast micropores in the range of 15–120 μm with a hairy fracture surface. The higher porosity would typically lead to a higher hydraulic conductivity, which will be helpful for diffusion and separation during the chemical process. The large amount of pits ranging from 0.5 to 10 μm in diameter were sustained in the parenchymal cells (Figure 1D(2)), which were used for nutrient transport and cell attachment in the live organism.^{31,76} These pits provide short diffusion distance while offering sufficient space due to the anisotropic and hierarchical structural feature, which is beneficial for enzyme immobilization and biocatalytic reactions.

Oxidation of the Bamboo Scaffold for Enzyme Immobilization. The delignified bamboo scaffold was oxidized using NaIO_4 to give the oxidized bamboo scaffold (OBS),^{47,62,77,78} which was then used for protein immobilization. The content of CHO (eq 2) was correlated to the reaction time.³³ Around 0.61 $\mu\text{mol}/\text{mg}$ CHO of OBS was observed

with 3 h of treatment (Table S2), which is ~ 2 -fold the literature result (0.32 $\mu\text{mol}/\text{mg}$).⁶² To quantify the efficiency of immobilization, fluorescein-5-maleimide-labeled BSA (F-BSA) was used as a model protein (Figures S3 and S4). As shown in Table S2, the loading amount of F-BSA per gram of OBS was 3.6–3.7 mg (eq 3). The loading amounts of F-BSA on different OBSs with varied contents of CHO were found similar (Table S2 and Figure S5), which almost reached the highest loading capacity (3.98 mg/g as the theoretical loading capacity, which was estimated based on the inner specific surface area of the OBS and the dimension of the BSA particle, eq 4). This result implied the excellent efficiency of the immobilization method for delignified bamboo. As shown in Figure 2 and Table S3, the protein loading capacity of the OBS

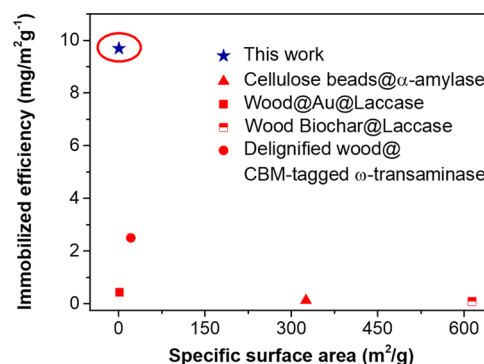


Figure 2. Comparison of immobilized efficiency versus specific surface area of different cellulose-based systems.^{36–39} BSA (MW: 66.5 kDa) was used for the measurement in this work.

($8.09 \text{ mg}/\text{m}^2 \cdot \text{g}^{-1}$) is 3–20 times that of delignified wood and other cellulose-based supports with comparable or much bigger specific surface area.^{36–39} Furthermore, when a high concentration of F-BSA (i.e., 1.0 mg/mL) was used, the protein loading was ~ 6 -fold that at low concentrations (0.1–0.4 mg/mL , Table S4 and Figure S6), indicating the diffusion rate as an important factor affecting the immobilization process. Similarly, when 1.0 mg/mL BGUs was used for immobilization, 4.4 ± 0.2 mg/g loading capacity was identified (Figure S7 and Table S4), which was close to the calculated theoretical capacity (4.8 mg/g , Table S4).

Activity of the BGU@OBS and Kinetic Analysis. To evaluate the activity of BGU@OBS, a chromogenic reaction with 4-nitrophenyl- β -D-glucuronide (pNPG) as the substrate was employed (Scheme 1 and Figure S8A,B). The reactions were carried out in phosphate buffer (pH 7.4) at room temperature, which is a common condition for BGU-based catalysis.^{54,57} As shown in Figure S8C–F, during the 15 min reaction, more than 86.8% conversion rate was achieved by BGU@OBS under shaking, while much lower conversion (24.5%) was observed without shaking, implying that the enzyme's function was largely sustained by comparing the conversion rate of the commercial enzyme. The reaction catalyzed by BGUs@OBS might be restricted by molecule diffusion. To further characterize the reaction kinetics, the initial reaction rate of BGU@OBS was assessed with increasing concentration of pNPG from 0.01 to 2.0 mM. The reactions with free enzyme (0.016 μg) were carried out with the same conditions for comparison. Different sizes of BGU@OBS with 5, 10, and 20 μg of enzyme were used in the assay for comparison. The Hanes–Woolf plotting analysis of pNPG

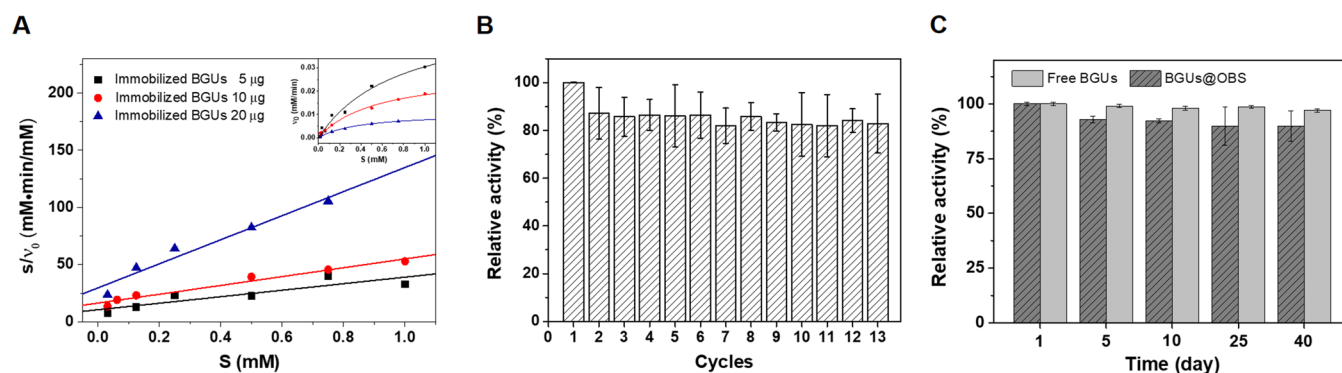


Figure 3. (A) Hanes–Woolf plots of experiments performed with OBS immobilized with different amounts of BGUs and the fitting of the Michaelis–Menten equation (insert). (B) Reusability of BGU@OBS. (C) Storage stability of free BGU and BGU@OBS ($\sim 4^\circ\text{C}$ for 40 days). The result of the first cycle in (B) and the first day in (C) was set as 100%. For (B) and (C), the enzymatic reactions were carried out in phosphate buffer (pH 7.4), at room temperature for 5 min. The error bars represent the standard deviation of the mean of triplicate samples.

hydrolysis showed a single straight line (Figure 3A), which supports a Michaelis–Menten behavior of BGU@OBS (Figure 3A, Insert). As shown in Table 1 and Figure S9, BGU@OBS

Table 1. Kinetic Parameters of Free BGU and Immobilized BGU^a

BGU	C_{BGU} (nmol/L)	K_m^b (mmol/L)	ν_{max}^c ($\mu\text{mol/L}\cdot\text{min}$)	K_{cat}^d (S^{-1})
free BGU/0.016 μg	0.24	0.24	3.30	229.28
BGU@OBS/5 μg	74.96	0.77	53.89	11.98
BGU@OBS/10 μg	149.93	0.54	28.47	3.16
BGU@OBS/20 μg	299.85	0.39	10.78	0.60

^aThe reaction rate was determined with 5 min reactions. In the assay, 0.016 μg of free BGU and 5–20 μg of immobilized BGU were used. ^b K_m = Michaelis–Menten constant in mM. ^c ν_{max} = maximum specific activity in $\mu\text{M}/\text{min}$. ^dThe turnover rate $K_{\text{cat}} = \nu_{\text{max}}/E$ (enzyme concentration).

showed a slower reaction kinetic behavior compared to that of the free enzyme in solution. BGU@OBS had a $\sim 3\times$ higher apparent enzyme–substrate affinity (K_m) and a $\sim 19\times$ lower catalytic activity (K_{cat}) than those of the free enzyme in solution. The results of the free enzyme we obtained are comparable with the published data.^{59,79,80} Generally, the biocatalytic processes involve both molecular and convective diffusion including substrate diffusion to catalytic sites and product diffusion back to the solution.^{39,81} Moreover, the density of BGU immobilized at different locations of the hierarchical scaffold should be different due to the gradient distribution of the vascular bundles from the inner skin to the outer skin.²⁸ In our system, molecular diffusion could be affected by the bamboo structure including their internal geometry.^{73–75} The rates of adsorption and desorption of small molecules (both the substrate and the product) by bamboo are related to the external diffusion coefficient and the internal resistance (due to the boundary layer, the diffusion in the materials, etc.).^{82,83} Under some conditions, the apparent diffusion coefficient could be positively correlated with the materials' thickness.⁸⁴ All these factors may cause a slightly decreased K_m value with a larger size of enzyme@OBS. Similarly, with plenty of micron-level pore sizes, the diffusion of enzymes could be dramatically affected by capillarity. The slower reaction rate displayed in the larger BGU@OBS sample further implied the effect of diffusional resistances on the enzymatic reactions (Table 1 and Figure S9B–D), which has

been described in heterogeneous enzyme systems.⁸¹ Other reasons that caused the activity decrease may include (1) less conformational flexibility of enzymes because of immobilization; (2) structural changes occurring during enzyme immobilization;⁸⁵ and (3) an unmixed solvent layer around the support surface, which is product-rich and substrate-depleted, hence leading to slower reaction kinetics.³⁹ More detailed studies are needed to further investigate these possible factors.

Reusability and Stability of the BGU@OBS. Free enzyme aggregation either during the reaction or storage is one major issue that limits enzymes' application.⁴⁴ Therefore, reusability and the improvement of enzymes' stability are important goals in the practical applications of enzyme immobilization. In this work, the same batch of BGU was used for enzyme immobilization and characterization to avoid batch-to-batch variations. As shown in Figure 3B,C, the BGU@OBS displayed excellent reusability and stability. The relative activity of immobilized BGU in the first run was set as 100%. After 13 cycles, $\sim 90\%$ of enzyme activity was maintained (Figure 3B). Figure 3C shows that $\sim 90\%$ of enzyme activity of immobilized BGU was maintained after more than 40 days of storage at 4°C . The slight activity decrease could be attributed to the leakage of BGU from the scaffold due to the degradation through ring opening during oxidation, which may disrupt the ordered structure of cellulose of the scaffold.⁸⁶

Flowing Reaction with a Single Enzyme and Bioseparation. In terms of synthetic and diagnostic applications of the immobilized enzymes, continuous flow biocatalysis is favored against the conventional bulk reaction due to continuous production, facilitated enzyme separation, and product isolation. The fast mass transfer and high permeability of the bamboo scaffold make the bamboo-based reactor an ideal system for a continuous system. Importantly, the interplay of either external or internal diffusion could be reduced.⁸¹

Moreover, the high-structured OBS may introduce multi-point interactions with the enzyme, which could minimize the enzyme leaching, which provides our system additional advantages for the flow reactions.⁴⁵ Therefore, a continuous flow reactor using BGU@OBS was constructed as shown in Figures 4A and S10. The whole system was an enclosed reactor vessel, and the flow rate was controlled using a syringe pump. As shown in Figure S11A, the conversion rate was increased

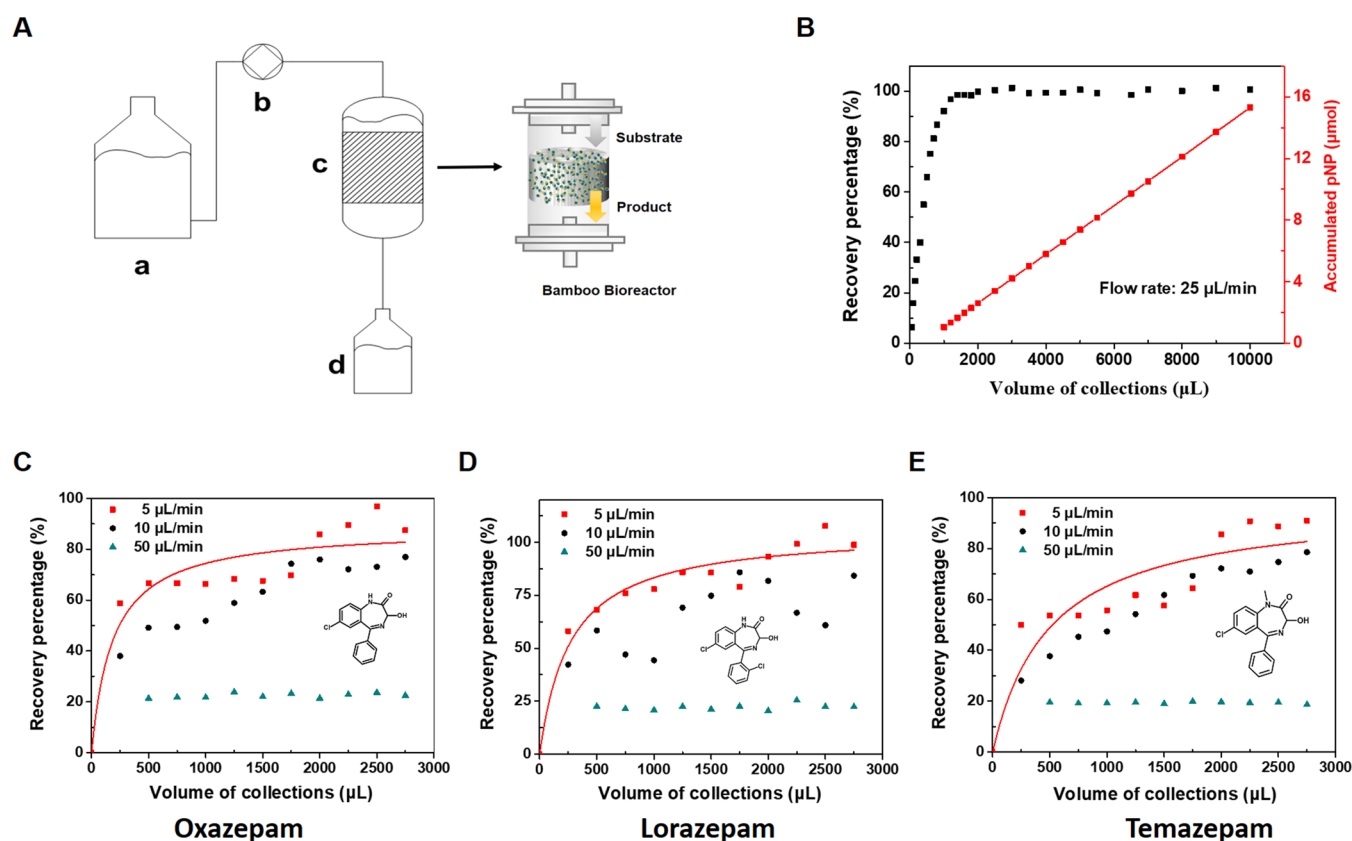


Figure 4. (A) Schematic illustration of the flow bioreactor: (a) substrate vessel, (b) pump, (c) bioreactor, and (d) product. (B) Recovery percentage (black curve) and accumulated product (red curve) as a function of volume of collections. The substrate (pNPG, 2.0 mM, 10 mL) was pumped to flow through the bioreactor with 25 $\mu\text{L}/\text{min}$ flow rate. The flow-through was collected and tested by UV spectroscopy. The recovery percentages were calculated by the conversion compared to free BGU (10 $\mu\text{g}/\text{mL}$). (C–E) Recovery percentage of oxazepam (C), lorazepam (D), and temazepam (E) hydrolyzed by BGU@OBS as a function of volume of collections at different flow rates. The flow reactor was executed by mounting one piece (diameter: 5.5 mm, height: 5 mm) of BGU@OBS. The spiked Surine mixture (glucuronides: 23.8 ppb, internal standard: 4.76 ppb) was pumped to run through the bioreactor at different flow rates (5, 10, 50 $\mu\text{L}/\text{min}$). Each fraction was collected every 250 μL and quenched with 160 μL of solvent with 5% FA in MeOH. The samples were transferred into a b-Gone Plus plate, centrifuged at 500g for 1 min, and then diluted using water (the volume of supernatants and water was 200 vs 600 μL) before LC-MS analysis. The molecule structures of the drugs are shown in the inset of (C–E).

with decreasing flow rate. The optimal flow rate that made >99% conversion was found as 25 $\mu\text{L}/\text{min}$. There is a diffusion process before the substrates contact with enzymes thoroughly. To test the flow volume of the process (i.e., dead volume), pNP was pumped to flow through the bioreactor until the concentration of collection was the same as the concentration used. As shown in Figure S11B, the dead volume was about 1 mL. Under the optimized conditions, the flow reaction was done for 20 μmol pNPG; around 15.3 μmol pNP (Figure 4B) could be accumulated after 6.7 h with 10 mL operation volume. Around 96.2% recovery rate was achieved. In addition, Figure S11C shows that ~88% of activity was maintained if the flow bioreactor was stored for 2 days at 4 $^{\circ}\text{C}$, while ~83% of the enzyme's activity was maintained after 7 weeks of storage at 4 $^{\circ}\text{C}$, demonstrating good reusability and stability of the OBS-based flow bioreactor.

In clinical and forensic laboratories, BGU is commonly used to hydrolyze glucuronic acid-conjugated drug metabolites present in different biological fluids. The enzyme hydrolysis efficiency and reproducibility are critical for analysis and diagnosis. We applied the BGU@OBS flow reactor to perform the hydrolysis of glucuronidated benzodiazepine drugs of abuse in synthetic urine. We chose three different representative benzodiazepine drugs: oxazepam, lorazepam, and

temazepam. As shown in Figure 4C–E, the BGU@OBS presented different recovery percentages at different rates. When the flow rate was set to 5 $\mu\text{L}/\text{min}$, the hydrolysis of glucuronides was above 90% within 1.5 mL of flow-through. The hydrolysis process of the BGU@OBS bioreactor was successfully applied for accurate detection of these three glucuronidated drugs, achieving over 90% recovery of glucuronides of glucuronidated benzodiazepines in Surine samples.

Flowing Reaction for Tandem Catalysis. Encouraged by the results with the single enzyme, we expanded the system to multienzyme reactions. Glucose oxidase (GOx) and horseradish peroxidase (HRP) were readily immobilized on separated OBSs to construct a dual-enzyme reactor, in which GOx@OBS first oxidized glucose to gluconolactone under the production of H_2O_2 . Then, H_2O_2 can be used by HRP@OBS as a cosubstrate for oxidation of the substrate ABTS. The functions of the two enzymes after immobilization were identified by the chromogenic assay. As shown in Figure S12, the green color of the solution was from the ABTS^+ , the product catalyzed by HRP@OBS in the presence of GOx@OBS and D-glucose, which indicated the functionality of the enzymes after immobilization. A flow-through cascade reaction was successfully executed by GOx@OBS and HRP@OBS as

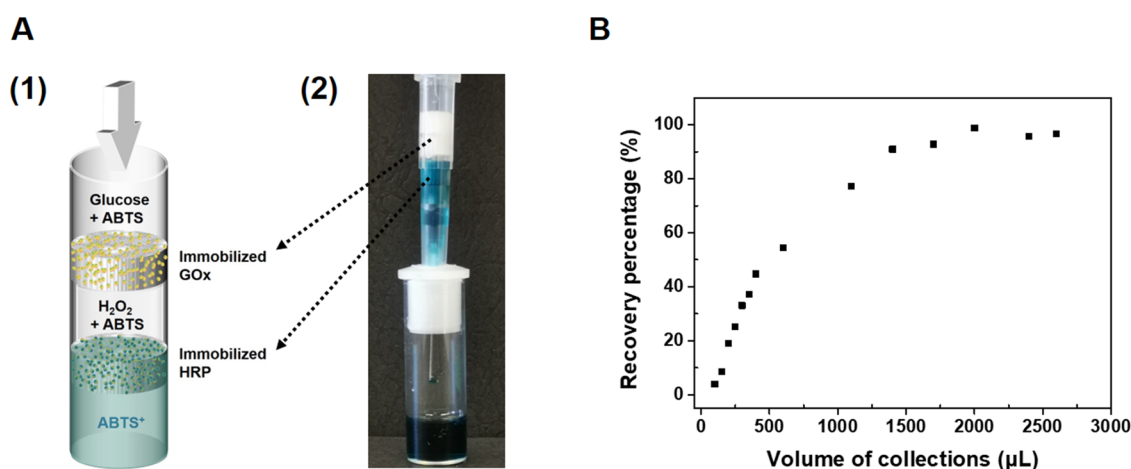


Figure 5. (A) Schematic diagram (1) and optical photograph (2) of the bioreactor for tandem catalysis with GOx@OBS and HRP@OBS. The flow reaction was first executed by mounting two pieces of GOx@OBS and then followed by two pieces of HRP@OBS. (B) Recovery percentage as a function of collection volume at 10 $\mu\text{L}/\text{min}$ flow rate. The substrate (D-glucose, 50 mM; ABTS, 2 mM; 3 mL) was pumped to run through the bioreactor; drops were collected and measured by UV-vis at 415 nm. The recovery percentages were calculated by the conversion compared to free GOx (1 nM) and HRP (2 nM) for 30 min.

shown in Figure 5A. Similar to the results obtained in the BGU-based bioreactor, we found that the recovery percentage reached $\sim 98\%$ after ~ 1.5 mL of flow-through (Figure 5B), which could be explained by the process of substrate diffusion before they contact with enzymes thoroughly. Figure 5B also implies that the immobilized GOx and HRP have good stability and reusability. Usually, lignin and hemicelluloses are degraded by H₂O₂ in other wood-based supports;^{87–89} no apparent deleterious effect was observed in our experiments, which implies that the delignified immobilized scaffolds have a predominant advantage when applied in this combined biosystem. Multienzyme-based biotransformations have experienced rapid growth for both scientific and industrial applications in recent decades.^{90–92} Conventionally, multi-enzymatic transformation is carried out in a one-pot reaction system. This approach has limitations due to potential cofactor competition, product mutual inhibition, etc.⁹⁰ Moreover, the separation of the multistep enzymatic reaction has disadvantages including high operation costs, instability of intermediate products, and low yields. Our results demonstrated that the OBS-based bioreactor could be transferred to multienzyme systems that may catalyze tandem reactions under a continuous flow setup for synthetic and other applications.

CONCLUSIONS

In summary, we successfully established a “green” technology of immobilized enzymes on a delignified bamboo scaffold and employed it to construct hierarchical flow-based bioreactors. After the efficient delignification and immobilization process, the three-dimensional (3D) anisotropic porous structure of the delignified bamboo scaffold was well-maintained, and excellent loading capacity was achieved. The conjugated biomaterials demonstrated sustained functionality, high stability and reusability. As a model enzyme, the immobilized BGU could be reused for at least 13 cycles with minimal activity lost and sustained its activity after storage for at least 7 weeks at 4 °C. We also demonstrated that the enzyme-immobilized bamboo scaffold could be readily constructed as flow reactors for both single and tandem catalysis. According to application demands, such a delignified scaffold could be functionalized by various enzymes and subsequently used in emerging applications. This

facile working scheme provides an economic, environmentally friendly, and efficient alternative for the enzyme-based synthesis and analysis. By choosing a specific bamboo, this approach could provide potential inspiration for immobilizing a large amount of biomolecules. Overall, this work reveals that functionalized bamboo has wide prospects to serve as a superior support for enzymes and other biomacromolecules’ application.

ASSOCIATED CONTENT

Supporting Information

The Supporting Information is available free of charge at <https://pubs.acs.org/doi/10.1021/acssuschemeng.2c00346>.

Characterizations of delignified bamboo; quantitative loading capacity of the enzyme immobilized on the OBS; activity test of BGU@OBS; and photographs and activity of flowing biocatalysis (PDF)

AUTHOR INFORMATION

Corresponding Authors

Yingwu Yin – Department of Chemical and Biochemical Engineering, College of Chemistry and Chemical Engineering, Xiamen University, Fujian 361005, China; orcid.org/0000-0002-9123-7761; Email: ywyin@xmu.edu.cn

Qian Wang – Department of Chemistry and Biochemistry, University of South Carolina, Columbia, South Carolina 29208, United States; orcid.org/0000-0002-2149-384X; Email: wang263@mailbox.sc.edu

Authors

Yihua Ren – Department of Chemical and Biochemical Engineering, College of Chemistry and Chemical Engineering, Xiamen University, Fujian 361005, China; Department of Chemistry and Biochemistry, University of South Carolina, Columbia, South Carolina 29208, United States

Libo Zhang – Department of Chemistry and Biochemistry, University of South Carolina, Columbia, South Carolina 29208, United States

Tao Sun – Department of Chemical and Biochemical Engineering, College of Chemistry and Chemical Engineering, Xiamen University, Fujian 361005, China

Complete contact information is available at:
<https://pubs.acs.org/10.1021/acssuschemeng.2c00346>

Author Contributions

§Y.R. and L.Z. contributed equally to this work.

Notes

The authors declare no competing financial interest.

ACKNOWLEDGMENTS

The β -glucuronidase was a gift from IMCS, Inc. (South Carolina). We would like to acknowledge the assistance of Amanda McGee and Dr. Nikki Sitasuwan of the IMCS Inc. for synthetic urine preparation and the quantitative analysis of glucuronidated drugs in synthetic urine systems. Q.W. and L.Z. acknowledge the partial support from the BDSHC initiative of the University of South Carolina and the NSF and SC EPSCoR/IDeA Program under NSF Award #OIA-1655740. The views, perspective, and content do not necessarily represent the official views of the SC EPSCoR/IDeA Program nor those of the NSF. Y.R. (201906310044) gratefully appreciates the financial support from the State Scholarship Fund of the China Scholarship Council (CSC).

REFERENCES

- (1) Yi, D.; Bayer, T.; Badenhorst, C. P. S.; Wu, S.; Doerr, M.; Höhne, M.; Bornscheuer, U. T. Recent trends in biocatalysis. *Chem. Soc. Rev.* **2021**, *50*, 8003–8049.
- (2) Cao, Y.; Li, X.; Ge, J. Enzyme Catalyst Engineering toward the Integration of Biocatalysis and Chemocatalysis. *Trends Biotechnol.* **2021**, *39*, 1173–1183.
- (3) Mulder, D. W.; Peters, J. W.; Raugei, S. Catalytic bias in oxidation-reduction catalysis. *Chem. Commun.* **2021**, *57*, 713–720.
- (4) Zhu, Y.; Huang, Z.; Chen, Q.; Wu, Q.; Huang, X.; So, P. K.; Shao, L.; Yao, Z.; Jia, Y.; Li, Z.; Yu, W.; Yang, Y.; Jian, A.; Sang, S.; Zhang, W.; Zhang, X. Continuous artificial synthesis of glucose precursor using enzyme-immobilized microfluidic reactors. *Nat. Commun.* **2019**, *10*, No. 4049.
- (5) Fernandez-Lopez, L.; Bartolome-Cabrero, R.; Rodriguez, M. D.; Dos Santos, C. S.; Rueda, N.; Fernandez-Lafuente, R. Stabilizing effects of cations on lipases depend on the immobilization protocol. *RSC Adv.* **2015**, *5*, 83868–83875.
- (6) Lima, G. V.; da Silva, M. R.; de Sousa Fonseca, T.; de Lima, L. B.; da Conceição Ferreira de Oliveira, M.; de Lemos, T. L. G.; Zampieri, D.; dos Santos, J. C. S.; Rios, N. S.; Gonçalves, L. R. B.; Molinari, F.; de Mattos, M. C. Chemoenzymatic synthesis of (S)-Pindolol using lipases. *Appl. Catal., A* **2017**, *546*, 7–14.
- (7) Pinheiro, M. P.; Rios, N. S.; de Sousa Fonseca, T.; de Aquino Bezerra, F.; Rodriguez-Castellon, E.; Fernandez-Lafuente, R.; de Mattos, M. C.; dos Santos, J. C. S.; Gonçalves, L. R. B. Kinetic resolution of drug intermediates catalyzed by lipase B from *Candida antarctica* immobilized on immodex-350. *Biotechnol. Prog.* **2018**, *34*, 878–889.
- (8) Galvão, W. S.; Pinheiro, B. B.; Gonçalves, L. R. B.; de Mattos, M. C.; Fonseca, T. S.; Regis, T.; Zampieri, D.; dos Santos, J. C. S.; Costa, L. S.; Correa, M. A.; Bohn, F.; Fachine, P. B. A. Novel nanohybrid biocatalyst: application in the kinetic resolution of secondary alcohols. *J. Mater. Sci.* **2018**, *53*, 14121–14137.
- (9) Virgen-Ortiz, J. J.; dos Santos, J. C. S.; Ortiz, C.; Berenguer-Murcia, A.; Barbosa, O.; Rodrigues, R. C.; Fernandez-Lafuente, R. Lecitase ultra: A phospholipase with great potential in biocatalysis. *Mol. Catal.* **2019**, *473*, No. 110405.
- (10) Dubey, N. C.; Tripathi, B. P. Nature Inspired Multienzyme Immobilization: Strategies and Concepts. *ACS Appl. Bio Mater.* **2021**, *4*, 1077–1114.
- (11) Manoel, E. A.; Pinto, M.; dos Santos, J. C. S.; Tacias-Pascacio, V. G.; Freire, D. M. G.; Pinto, J. C.; Fernandez-Lafuente, R. Design of a core-shell support to improve lipase features by immobilization. *RSC Adv.* **2016**, *6*, 62814–62824.
- (12) Gericke, M.; Trygg, J.; Fardim, P. Functional cellulose beads: preparation, characterization, and applications. *Chem. Rev.* **2013**, *113*, 4812–4836.
- (13) Alavijeh, M. K.; Meyer, A. S.; Gras, S. L.; Kentish, S. E. Improving β -Galactosidase-Catalyzed Transglycosylation Yields by Cross-Linked Layer-by-Layer Enzyme Immobilization. *ACS Sustainable Chem. Eng.* **2020**, *8*, 16205–16216.
- (14) Zebda, A.; Gondran, C.; Le Goff, A.; Holzinger, M.; Cinquin, P.; Cosnier, S. Mediatorless high-power glucose biofuel cells based on compressed carbon nanotube-enzyme electrodes. *Nat. Commun.* **2011**, *2*, No. 370.
- (15) Liang, S.; Wu, X.-L.; Xiong, J.; Zong, M.-H.; Lou, W.-Y. Metal-organic frameworks as novel matrices for efficient enzyme immobilization: An update review. *Coord. Chem. Rev.* **2020**, *406*, No. 213149.
- (16) Zhang, L.; Xu, Y.; Makris, T. M.; Wang, Q. Enhanced Arylamine N-Oxygenase Activity of Polymer-Enzyme Assemblies by Facilitating Electron-Transferring Efficiency. *Biomacromolecules* **2018**, *19*, 918–925.
- (17) Lu, L.; Zhang, L.; Yuan, L.; Zhu, T.; Chen, W.; Wang, G.; Wang, Q. Artificial Cellulosome Complex from the Self-Assembly of Ni-NTA-Functionalized Polymeric Micelles and Cellulases. *ChemBioChem* **2019**, *20*, 1394–1399.
- (18) Gao, Y.; Luo, Q.; Qiao, S.; Wang, L.; Dong, Z.; Xu, J.; Liu, J. Enzymatically regulating the self-healing of protein hydrogels with high healing efficiency. *Angew. Chem., Int. Ed.* **2014**, *53*, 9343–9346.
- (19) Shang, X.; Chen, H.; Castagnola, V.; Liu, K.; Boselli, L.; Petseva, V.; Yu, L.; Xiao, L.; He, M.; Wang, F.; Dawson, K. A.; Fan, J. Unusual zymogen activation patterns in the protein corona of Ca-zeolites. *Nat. Catal.* **2021**, *4*, 607–614.
- (20) Wang, K.; Zhao, L.; Li, T.; Wang, Q.; Ding, Z.; Dong, W. Selective Immobilization of His-Tagged Phosphomannose Isomerase on Ni Chelated Nanoparticles with Good Reusability and Activity. *ChemBioChem* **2022**, *23*, No. e202100497.
- (21) Thomas, B.; Raj, M. C.; B, A. K.; H, R. M.; Joy, J.; Moores, A.; Drisko, G. L.; Sanchez, C. Nanocellulose, a Versatile Green Platform: From Biosources to Materials and Their Applications. *Chem. Rev.* **2018**, *118*, 11575–11625.
- (22) Moon, R. J.; Martini, A.; Nairn, J.; Simonsen, J.; Youngblood, J. Cellulose nanomaterials review: structure, properties and nanocomposites. *Chem. Soc. Rev.* **2011**, *40*, 3941–3994.
- (23) Habibi, Y.; Lucia, L. A.; Rojas, O. J. Cellulose nanocrystals: chemistry, self-assembly, and applications. *Chem. Rev.* **2010**, *110*, 3479–3500.
- (24) Benítez-Mateos, A. I.; Contente, M. L.; Velasco-Lozano, S.; Paradisi, F.; López-Gallego, F. Self-Sufficient Flow-Biocatalysis by Coimmobilization of Pyridoxal 5'-Phosphate and ω -Transaminases onto Porous Carriers. *ACS Sustainable Chem. Eng.* **2018**, *6*, 13151–13159.
- (25) Xiu, G.-h.; Jiang, L.; Li, P. Mass-Transfer Limitations for Immobilized Enzyme-Catalyzed Kinetic Resolution of Racemate in a Batch Reactor. *Ind. Eng. Chem. Res.* **2000**, *39*, 4054–4062.
- (26) Basso, A.; Serban, S. Industrial applications of immobilized enzymes—A review. *Mol. Catal.* **2019**, *479*, No. 110607.
- (27) Jas, G.; Kirschning, A. Continuous flow techniques in organic synthesis. *Chem. - Eur. J.* **2003**, *9*, 5708–5723.
- (28) Wegst, U. G. K.; Bai, H.; Saiz, E.; Tomsia, A. P.; Ritchie, R. O. Bioinspired structural materials. *Nat. Mater.* **2015**, *14*, 23–36.
- (29) Li, T.; Song, J.; Zhao, X.; Yang, Z.; Pastel, G.; Xu, S.; Jia, C.; Dai, J.; Chen, C.; Gong, A.; Jiang, F.; Yao, Y.; Fan, T.; Yang, B.; Wägberg, L.; Yang, R.; Hu, L. Anisotropic, lightweight, strong, and super thermally insulating nanowood with naturally aligned nanocellulose. *Sci. Adv.* **2018**, *4*, No. eaar3724.
- (30) de Sá, D. S.; de Andrade Bustamante, R.; Rocha, C. E. R.; da Silva, V. D.; da Rocha Rodrigues, E. J.; Müller, C. D. B.; Ghavami, K.; Massi, A.; Pandoli, O. G. Fabrication of Lignocellulose-Based Microreactors: Copper-Functionalized Bamboo for Continuous-

Flow CuAAC Click Reactions. *ACS Sustainable Chem. Eng.* **2019**, *7*, 3267–3273.

(31) Berglund, L. A.; Burgert, I. Bioinspired Wood Nanotechnology for Functional Materials. *Adv. Mater.* **2018**, *30*, No. 1704285.

(32) Jin, K.; Kong, L.; Liu, X.; Jiang, Z.; Tian, G.; Yang, S.; Feng, L.; Ma, J. Understanding the Xylan Content for Enhanced Enzymatic Hydrolysis of Individual Bamboo Fiber and Parenchyma Cells. *ACS Sustainable Chem. Eng.* **2019**, *7*, 18603–18611.

(33) Huang, C.; Fang, G.; Zhou, Y.; Du, X.; Yu, L.; Meng, X.; Li, M.; Yoo, C. G.; Chen, B.; Zhai, S.; Guan, Q.; Yong, Q.; Ragauskas, A. J. Increasing the Carbohydrate Output of Bamboo Using a Combinatorial Pretreatment. *ACS Sustainable Chem. Eng.* **2020**, *8*, 7380–7393.

(34) Liu, J.; Yu, P.; Wang, D.; Chen, Z.; Cui, Q.; Hu, B.; Zhang, D.; Li, Y.; Chu, H.; Li, J. Wood-Derived Hybrid Scaffold with Highly Anisotropic Features on Mechanics and Liquid Transport toward Cell Migration and Alignment. *ACS Appl. Mater. Interfaces* **2020**, *12*, 17957–17966.

(35) Li, T.; Liu, H.; Zhao, X.; Chen, G.; Dai, J.; Pastel, G.; Jia, C.; Chen, C.; Hitz, E.; Siddhartha, D.; Yang, R.; Hu, L. Scalable and Highly Efficient Mesoporous Wood-Based Solar Steam Generation Device: Localized Heat, Rapid Water Transport. *Adv. Funct. Mater.* **2018**, *28*, No. 1707134.

(36) Roberts, A. D.; Payne, K. A. P.; Cosgrove, S.; Tilakaratra, V.; Penafiel, I.; Finnigan, W.; Turner, N. J.; Scrutton, N. S. Enzyme immobilisation on wood-derived cellulose scaffolds via carbohydrate-binding module fusion constructs. *Green Chem.* **2021**, *23*, 4716–4732.

(37) Li, N.; Xia, Q.; Niu, M.; Ping, Q.; Xiao, H. Immobilizing Laccase on Different Species Wood Biochar to Remove the Chlorinated Biphenyl in Wastewater. *Sci. Rep.* **2018**, *8*, No. 13947.

(38) Sun, Z.; Su, H.; Zhong, Y.; Xu, H.; Wang, B.; Zhang, L.; Sui, X.; Feng, X.; Mao, Z. Preparation of 3D porous cellulose-chitosan hybrid gel microspheres by alkaline urea system for enzyme immobilization. *Polym. Adv. Technol.* **2022**, *33*, 546–555.

(39) Goldhahn, C.; Taut, J. A.; Schubert, M.; Burgert, I.; Chanana, M. Enzyme immobilization inside the porous wood structure: a natural scaffold for continuous-flow biocatalysis. *RSC Adv.* **2020**, *10*, 20608–20619.

(40) Guisán, J. Aldehyde-agarose gels as activated supports for immobilization-stabilization of enzymes. *Enzyme Microb. Technol.* **1988**, *10*, 375–382.

(41) Morellon-Sterling, R.; Carballares, D.; Arana-Peña, S.; Siar, E.-H.; Braham, S. A.; Fernandez-Lafuente, R. Advantages of Supports Activated with Divinyl Sulfone in Enzyme Coimmobilization: Possibility of Multipoint Covalent Immobilization of the Most Stable Enzyme and Immobilization via Ion Exchange of the Least Stable Enzyme. *ACS Sustainable Chem. Eng.* **2021**, *9*, 7508–7518.

(42) Rodrigues, R. C.; Berenguer-Murcia, A.; Carballares, D.; Morellon-Sterling, R.; Fernandez-Lafuente, R. Stabilization of enzymes via immobilization: Multipoint covalent attachment and other stabilization strategies. *Biotechnol. Adv.* **2021**, *52*, No. 107821.

(43) Zahirinejad, S.; Hemmati, R.; Homaei, A.; Dinari, A.; Hosseinkhani, S.; Mohammadi, S.; Vianello, F. Nano-organic supports for enzyme immobilization: Scopes and perspectives. *Colloids Surf., B* **2021**, *204*, No. 111774.

(44) Sanchez, A.; Cruz, J.; Rueda, N.; dos Santos, J. C. S.; Torres, R.; Ortiz, C.; Villalonga, R.; Fernandez-Lafuente, R. Inactivation of immobilized trypsin under dissimilar conditions produces trypsin molecules with different structures. *RSC Adv.* **2016**, *6*, 27329–27334.

(45) Nunes, Y. L.; de Menezes, F. L.; de Sousa, I. G.; Cavalcante, A. L. G.; Cavalcante, F. T. T.; da Silva Moreira, K.; de Oliveira, A. L. B.; Mota, G. F.; da Silva Souza, J. E.; de Aguiar Falcao, I. R.; Rocha, T. G.; Valerio, R. B. R.; Fechine, P. B. A.; de Souza, M. C. M.; dos Santos, J. C. S. Chemical and physical Chitosan modification for designing enzymatic industrial biocatalysts: How to choose the best strategy? *Int. J. Biol. Macromol.* **2021**, *181*, 1124–1170.

(46) Rodrigues, D. S.; Mendes, A. A.; Adriano, W. S.; Gonçalves, L. R. B.; Giordano, R. L. C. Multipoint covalent immobilization of microbial lipase on chitosan and agarose activated by different methods. *J. Mol. Catal. B: Enzym.* **2008**, *51*, 100–109.

(47) Luo, X.; Xia, J.; Jiang, X.; Yang, M.; Liu, S. Cellulose-Based Strips Designed Based on a Sensitive Enzyme Colorimetric Assay for the Low Concentration of Glucose Detection. *Anal. Chem.* **2019**, *91*, 15461–15468.

(48) Jia, Y.; Li, J. Molecular assembly of Schiff Base interactions: construction and application. *Chem. Rev.* **2015**, *115*, 1597–1621.

(49) Ghasemi, M.; Minier, M. J.; Tatoulian, M.; Chehimi, M. M.; Arefi-Khonsari, F. Ammonia plasma treated polyethylene films for adsorption or covalent immobilization of trypsin: quantitative correlation between X-ray photoelectron spectroscopy data and enzyme activity. *J. Phys. Chem. B* **2011**, *115*, 10228–10238.

(50) Hermanson, G. T. The Reactions of Bioconjugation. In *Bioconjugate Techniques*, 3rd ed.; Audet, J.; Preap, M., Eds.; Elsevier, 2013; pp 229–258.

(51) Korecká, L.; Bilková, Z.; Holèapek, M.; Královský, J.; Beneš, M.; Lenfeld, J.; Minc, N.; Cecal, R.; Viovy, J. L.; Przybylski, M. Utilization of newly developed immobilized enzyme reactors for preparation and study of immunoglobulin G fragments. *J. Chromatogr. B* **2004**, *808*, 15–24.

(52) Neira, H. D.; Herr, A. E. Kinetic Analysis of Enzymes Immobilized in Porous Film Arrays. *Anal. Chem.* **2017**, *89*, 10311–10320.

(53) Kobayashi, H.; Suzuki, H. Kinetic studies of alpha-galactosidase-containing mold pellets on PNPG hydrolysis. *Biotechnol. Bioeng.* **1976**, *18*, 37–51.

(54) Taylor, M. R.; Flannigan, K. L.; Rahim, H.; Mohamad, A.; Lewis, I. A.; Hirota, S. A.; Greenway, S. C. Vancomycin relieves mycophenolate mofetil-induced gastrointestinal toxicity by eliminating gut bacterial beta-glucuronidase activity. *Sci. Adv.* **2019**, *5*, No. eaax2358.

(55) Awolade, P.; Cele, N.; Kerru, N.; Gummidu, L.; Oluwakemi, E.; Singh, P. Therapeutic significance of beta-glucuronidase activity and its inhibitors: A review. *Eur. J. Med. Chem.* **2020**, *187*, No. 111921.

(56) Ding, Y.; Peng, M.; Zhang, T.; Tao, J. S.; Cai, Z. Z.; Zhang, Y. Quantification of conjugated metabolites of drugs in biological matrices after the hydrolysis with beta-glucuronidase and sulfatase: a review of bio-analytical methods. *Biomed. Chromatogr.* **2013**, *27*, 1280–1295.

(57) Cheng, T. C.; Roffler, S. R.; Tzou, S. C.; Chuang, K. H.; Su, Y. C.; Chuang, C. H.; Kao, C. H.; Chen, C. S.; Harn, I. H.; Liu, K. Y.; Cheng, T. L.; Leu, Y. L. An activity-based near-infrared glucuronide trapping probe for imaging beta-glucuronidase expression in deep tissues. *J. Am. Chem. Soc.* **2012**, *134*, 3103–3110.

(58) Jain, S.; Drendel, W. B.; Chen, Z. W.; Mathews, F. S.; Sly, W. S.; Grubb, J. H. Structure of human beta-glucuronidase reveals candidate lysosomal targeting and active-site motifs. *Nat. Struct. Mol. Biol.* **1996**, *3*, 375–381.

(59) Islam, M. R.; Tomatsu, S.; Shah, G. N.; Grubb, J. H.; Jain, S.; Sly, W. S. Active site residues of human beta-glucuronidase. Evidence for Glu(540) as the nucleophile and Glu(451) as the acid-base residue. *J. Biol. Chem.* **1999**, *274*, 23451–23455.

(60) Liu, D.-M.; Dong, C. Recent advances in nano-carrier immobilized enzymes and their applications. *Process Biochem.* **2020**, *92*, 464–475.

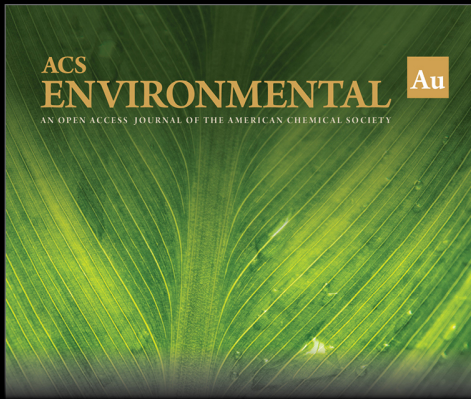
(61) Hou, D.; Li, T.; Chen, X.; He, S.; Dai, J.; Mofid, S. A.; Hou, D.; Iddya, A.; Jassby, D.; Yang, R.; Hu, L.; Ren, Z. J. Hydrophobic nanostructured wood membrane for thermally efficient distillation. *Sci. Adv.* **2019**, *5*, No. eaaw3203.

(62) Cai, Q.; Yang, S.; Zhang, C.; Li, Z.; Li, X.; Shen, Z.; Zhu, W. Facile and Versatile Modification of Cotton Fibers for Persistent Antibacterial Activity and Enhanced Hygroscopicity. *ACS Appl. Mater. Interfaces* **2018**, *10*, 38506–38516.

(63) Leguy, J.; Nishiyama, Y.; Jean, B.; Heux, L. Ultrastructural Characterization of the Core–Shell Structure of a Wide Range of Periodate-Oxidized Cellulose from Different Native Sources by Solid-State ¹³C CP-MAS NMR. *ACS Sustainable Chem. Eng.* **2019**, *7*, 412–420.

(64) Winborn, J.; Kerrigan, S. Stability and Hydrolysis of Desomorphine-Glucuronide. *J. Anal. Toxicol.* **2019**, *43*, 536–542.

- (65) Collins, R. A.; Ng, T. B.; Fong, W. P.; Wan, C. C.; Yeung, H. W. Inhibition of glycohydrolase enzymes by aqueous extracts of Chinese medicinal herbs in a microplate format. *IUBMB Life* **1997**, *42*, 1163–1169.
- (66) Frey, M.; Widner, D.; Segmehl, J. S.; Casdorff, K.; Keplinger, T.; Burgert, I. Delignified and Densified Cellulose Bulk Materials with Excellent Tensile Properties for Sustainable Engineering. *ACS Appl. Mater. Interfaces* **2018**, *10*, 5030–5037.
- (67) Poppius-Levlin, K.; Jääskeläinen, A. S.; Seisto, A.; Fuhrmann, A. Peracids in Kraft Pulp Bleaching: Past, Present, and Future. In *Lignin: Historical, Biological, and Materials Perspectives*; Glasser, W. G.; Northey, R. A.; Schultz, T. P., Eds.; American Chemical Society, 1999; Vol. 742, pp 471–489.
- (68) Sun, J.; Guo, H.; Schädli, G. N.; Tu, K.; Schär, S.; Schwarze, F.; Panzarasa, G.; Ribera, J.; Burgert, I. Enhanced mechanical energy conversion with selectively decayed wood. *Sci. Adv.* **2021**, *7*, No. eabd9138.
- (69) Chen, C.; Li, Z.; Mi, R.; Dai, J.; Xie, H.; Pei, Y.; Li, J.; Qiao, H.; Tang, H.; Yang, B.; Hu, L. Rapid Processing of Whole Bamboo with Exposed, Aligned Nanofibrils toward a High-Performance Structural Material. *ACS Nano* **2020**, *14*, 5194–5202.
- (70) Ge, S.; Ma, N. L.; Jiang, S.; Ok, Y. S.; Lam, S. S.; Li, C.; Shi, S. Q.; Nie, X.; Qiu, Y.; Li, D.; Wu, Q.; Tsang, D. C. W.; Peng, W.; Sonne, C. Processed Bamboo as a Novel Formaldehyde-Free High-Performance Furniture Biocomposite. *ACS Appl. Mater. Interfaces* **2020**, *12*, 30824–30832.
- (71) Sun, S. L.; Wen, J. L.; Ma, M. G.; Sun, R. C. Successive alkali extraction and structural characterization of hemicelluloses from sweet sorghum stem. *Carbohydr. Polym.* **2013**, *92*, 2224–2231.
- (72) Xia, Q.; Chen, C.; Li, T.; He, S.; Gao, J.; Wang, X.; Hu, L. Solar-assisted fabrication of large-scale, patternable transparent wood. *Sci. Adv.* **2021**, *7*, No. eabd7342.
- (73) Lian, C.; Liu, R.; Xiufang, C.; Zhang, S.; Luo, J.; Yang, S.; Liu, X.; Fei, B. Characterization of the pits in parenchyma cells of the moso bamboo [*Phyllostachys edulis* (Carr.) J. Houz.] culm. *Holzforchung* **2019**, *73*, 629–636.
- (74) Yu, Y.; Huang, Y.; Zhang, Y.; Liu, R.; Meng, F.; Yu, W. The reinforcing mechanism of mechanical properties of bamboo fiber bundle-reinforced composites. *Polym. Compos.* **2019**, *40*, 1463–1472.
- (75) Tang, T.; Zhang, B.; Liu, X.; Wang, W.; Chen, X.; Fei, B. Synergistic effects of tung oil and heat treatment on physicochemical properties of bamboo materials. *Sci. Rep.* **2019**, *9*, No. 12824.
- (76) Chen, C.; Kuang, Y.; Zhu, S.; Burgert, I.; Keplinger, T.; Gong, A.; Li, T.; Berglund, L.; Eichhorn, S. J.; Hu, L. Structure–property–function relationships of natural and engineered wood. *Nat. Rev. Mater.* **2020**, *5*, 642–666.
- (77) Buist, G. J.; Bunton, C. A.; Lomas, J. The mechanism of oxidation of α -glycols by periodic acid. Part VI. Oxidation of pinacol at pH 0–6. *J. Chem. Soc. B* **1966**, *0*, 1094–1099.
- (78) Dryhurst, G. Periodate Oxidation of Diol and other Functional Groups. Analytical and Structural Applications. In *Carbohydrate Research*; Belcher, R.; Anderson, D. M. W., Eds.; Elsevier: Pergamon, London/New York, 1971; Vol. 19, p 144.
- (79) Glaser, J. H.; Conrad, H. E. Multiple kinetic forms of beta-glucuronidase. *J. Biol. Chem.* **1980**, *255*, 1879–1884.
- (80) Eudes, A.; Mouille, G.; Thevenin, J.; Goyallon, A.; Minic, Z.; Jouanin, L. Purification, cloning and functional characterization of an endogenous beta-glucuronidase in *Arabidopsis thaliana*. *Plant Cell Physiol.* **2008**, *49*, 1331–1341.
- (81) Engasser, J.-M.; Horvath, C. Diffusion and Kinetics with Immobilized Enzymes. In *Applied Biochemistry and Bioengineering*; L, B. W., Jr.; Katchalski-Katzir, E.; Goldstein, L., Eds.; Elsevier, 1976; Vol. 1, pp 127–220.
- (82) Chen, Y.; Choong, E. T.; Wetzal, D. M. Evaluation of diffusion coefficient and surface emission coefficient by an optimization technique. *Wood Fiber Sci.* **1995**, *27*, 178–182. <https://wfs.swst.org/index.php/wfs/article/view/281>.
- (83) Siau, J. F.; Avramidis, S. The surface emission coefficient of wood. *Wood Fiber Sci.* **1996**, *28*, 178–185.
- (84) Avramidis, S.; Siau, J. F. An investigation of the external and internal resistance to moisture diffusion in wood. *Wood Sci. Technol.* **1987**, *21*, 249–256.
- (85) Petry, I.; Ganesan, A.; Pitt, A.; Moore, B. D.; Halling, P. J. Proteomic methods applied to the analysis of immobilized biocatalysts. *Biotechnol. Bioeng.* **2006**, *95*, 984–991.
- (86) Chimpibul, W.; Nakaji-Hirabayashi, T.; Yuan, X.; Matsumura, K. Controlling the degradation of cellulose scaffolds with Malaprade oxidation for tissue engineering. *J. Mater. Chem. B* **2020**, *8*, 7904–7913.
- (87) Zhu, M.; Song, J.; Li, T.; Gong, A.; Wang, Y.; Dai, J.; Yao, Y.; Luo, W.; Henderson, D.; Hu, L. Highly Anisotropic, Highly Transparent Wood Composites. *Adv. Mater.* **2016**, *28*, 5181–5187.
- (88) Li, Y.; Fu, Q.; Rojas, R.; Yan, M.; Lawoko, M.; Berglund, L. Lignin-Retaining Transparent Wood. *ChemSusChem* **2017**, *10*, 3445–3451.
- (89) Li, T.; Zhang, X.; Lacey, S. D.; Mi, R.; Zhao, X.; Jiang, F.; Song, J.; Liu, Z.; Chen, G.; Dai, J.; Yao, Y.; Das, S.; Yang, R.; Briber, R. M.; Hu, L. Cellulose ionic conductors with high differential thermal voltage for low-grade heat harvesting. *Nat. Mater.* **2019**, *18*, 608–613.
- (90) Cai, T.; Sun, H.; Qiao, J.; Zhu, L.; Zhang, F.; Zhang, J.; Tang, Z.; Wei, X.; Yang, J.; Yuan, Q.; Wang, W.; Yang, X.; Chu, H.; Wang, Q.; You, C.; Ma, H.; Sun, Y.; Li, Y.; Li, C.; Jiang, H.; Wang, Q.; Ma, Y. Cell-free chemoenzymatic starch synthesis from carbon dioxide. *Science* **2021**, *373*, 1523–1527.
- (91) Hwang, E. T.; Lee, S. Multienzymatic Cascade Reactions via Enzyme Complex by Immobilization. *ACS Catal.* **2019**, *9*, 4402–4425.
- (92) Zhang, L.; Wang, Q. Harnessing P450 Enzyme for Biotechnology and Synthetic Biology. *ChemBioChem* **2022**, *23*, No. e202100439.



ACS
ENVIRONMENTAL Au
AN OPEN ACCESS JOURNAL OF THE AMERICAN CHEMICAL SOCIETY

Editor-in-Chief: **Prof. Shelley D. Minteer**, University of Utah, USA

Deputy Editor:
Prof. Xiang-Dong Li
Hong Kong Polytechnic University, China

Open for Submissions 

pubs.acs.org/environau  ACS Publications
Most Trusted. Most Cited. Most Read.